Molecular Architecture of DesI: A Key Enzyme in the Biosynthesis of Desosamine[†,‡]

E. Sethe Burgie and Hazel M. Holden*

Department of Biochemistry, University of Wisconsin, Madison, Wisconsin 53706

Received April 20, 2007; Revised Manuscript Received May 29, 2007

ABSTRACT: Desosamine is a 3-(dimethylamino)-3,4,6-trideoxyhexose found, for example, in such macrolide antibiotics as erthyromycin, azithromycin, and clarithromycin. The efficacies of these macrolide antibiotics are markedly reduced in the absence of desosamine. In the bacterium *Streptomyces venezuelae*, six enzymes are required for the production of dTDP-desosamine. The focus of this X-ray crystallographic analysis is the third enzyme in the pathway, a PLP-dependent aminotransferase referred to as DesI. The structure of DesI was solved in complex with its product, dTDP-4-amino-4,6-dideoxyglucose, to a nominal resolution of 2.1 Å. Each subunit of the dimeric enzyme contains 12 α-helices and 14 β-strands. Three cis-peptides are observed in each subunit, Phe 330, Pro 332, and Pro 339. The two active sites of the enzyme are located in clefts at the subunit/subunit interface. Electron density corresponding to the bound product clearly demonstrates a covalent bond between the amino group of the product and C-4′ of the PLP cofactor. Interestingly, there are no hydrogen-bonding interactions between the protein and the dideoxyglucosyl group of the product (within 3.2 Å). The only other sugar-modifying aminotransferase whose structure is known in the presence of product is PseC from *Helicobacter pylori*. This enzyme, as opposed to DesI, catalyzes amino transfer to the axial position of the sugar. A superposition of the two active sites for these proteins reveals that the major differences in ligand binding occur in the orientations of the deoxyglucosyl and phosphoryl groups. Indeed, the nearly 180° difference in hexose orientation explains the equatorial versus axial amino transfer exhibited by DesI and PseC, respectively.

Macrolide antibiotics, such as erythromycin, azithromycin, clarithromycin, and roxithromycin, constitute a well-established class of antimicrobial agents used for the treatment of respiratory tract, urinary tract, skin, and soft tissue infections. These drugs function by binding to bacterial ribosomes and inhibiting protein synthesis (*1*−*3*). Clinically, macrolides demonstrate a wider antimicrobial spectrum than penicillin and have been shown to be effective against *Streptococcus pneumoniae*, *Streptococcus pyogenes*, *Staphylococcus* species, *Mycoplasma pneumoniae*, *Legionella pneumophila*, *Chlamydophila pneumoniae*, *Moraxella catarrhalis*, and *Haemophilus influenzae* (*4*). As the name implies, these drugs contain a macrolide or lactone ring, which can be 14-, 15-, or 16-membered. Attached to these rings are a number of unusual 2,6-dideoxy- or 2,3(4),6-trideoxysugars (*5*, *6*). One of these is desosamine[1], a 3-(dimethylamino)-3,4,6-trideoxyglucose that is essential for the bactericidal activity of erythromycin and many of its derivatives (*7*). It is appended to the macrolide rings of the antibiotics through the action of a glycosyltransferase with dTDP-desosamine serving as the sugar donor.

Six enzymes are required for the production of dTDP-desosamine in *Streptomyces venezuelae* (Scheme 1). As is common in many biosynthetic pathways for unusual sugars, dTDP-desosamine production begins with the attachment of α-D-glucose-1-phosphate to dTMP (in *S. venezuelae*, this reaction is catalyzed by DesIII). In the next step, the 6′-hydroxyl group of the sugar is removed, and the 4′-hydroxyl group is oxidized to a keto-functionality through the action of a dehydratase referred to as DesIV. The focus of this investigation is DesI, which catalyzes the next step in the pathway, namely, the PLP-dependent amination of the sugar C-4′ position. This ping−pong reaction first requires the conversion of PLP to PMP using glutamate as the nitrogen source, followed by amination of the sugar substrate. In the reaction catalyzed by DesI, the resulting amino group lies in the equatorial position. Following this amination by DesI, the next enzyme in the pathway, DesII, removes the amino group at the C-4′ position and oxidizes the C-3′ hydroxyl group to a keto moiety. As indicated in Scheme 1, there is a second PLP-dependent enzyme in the pathway, DesV, that adds an amino group equatorially to C-3′. Not surprisingly, given their similar modes of action and similar substrates, DesI and DesV demonstrate an amino acid sequence identity of 34.2%. From previous work in our laboratory, the three-dimensional folds of both DesIV and DesV are now known (*8*, *9*). The structure of DesV revealed the manner in which it accommodates either the internal aldimine form of

[†] This research was supported by an NIH grant (DK47814 to H.M.H.).

[‡] X-ray coordinates have been deposited in the Research Collaboratory for Structural Bioinformatics, Rutgers University, New Brunswick, NJ (accession no. 2PO3).

* To whom correspondence should be addressed. Phone: 608-262-4988. Fax: 608-262-1319. E-mail: Hazel_Holden@biochem.wisc.edu.

[1] Abbreviations: desosamine, 3-(dimethylamino)-3,4,6-trideoxyglucose; dTDP, deoxythymidine diphosphoglucose; dTTP, deoxythymidine 5′-triphosphate; ESI-MS, electrospray ionization mass spectrometry; HEPPS, 3-[4-(2-hydroxyethyl)-1-piperazinyl]propanesulfonic acid.

10.1021/bi700751d CCC: $37.00
Published on Web 07/13/2007

Scheme 1

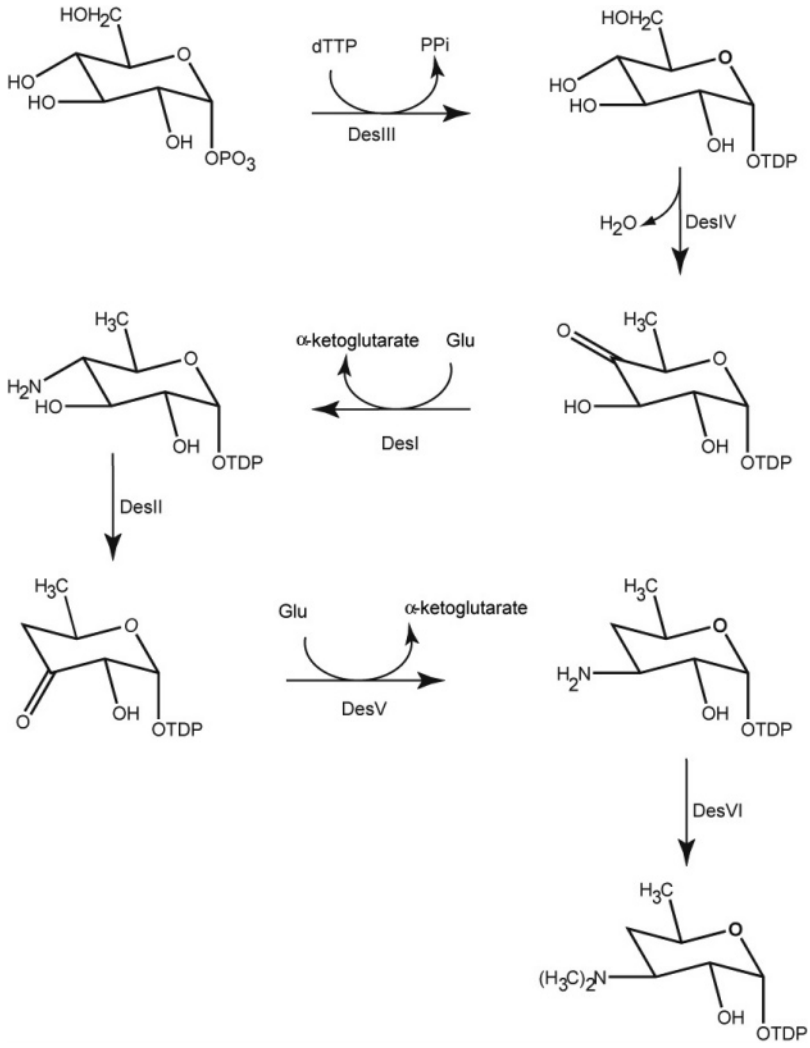

PLP or the ketimine intermediate of glutamate. It was not possible, however, to solve the structure of DesV with a bound dTDP-sugar ligand. In the present investigation, crystals of DesI with bound product were obtained and a high-resolution X-ray analysis conducted. This investigation reveals the manner in which the ligand is accommodated within the active site pocket. The only other sugar-modifying aminotransferase whose structure has been solved with a bound sugar ligand is PseC, an enzyme from *Helicobacter pylori* that is involved in the biosynthesis of pseudaminic acid (*10*).

In recent years, the enzymes involved in the production of unusual di- and tri-deoxysugars such as desosamine have attracted significant research attention due in part to the increasing concern over microbial resistance to current antibiotics, including the macrolides. As reported by the Centers for Disease Control and Prevention, nearly 2 million patients in the United States will acquire an infection in the hospital each year, approximately 90,000 of these patients will die as a direct result of their infection, and more than 70% of the bacteria causing these infections are resistant to at least one of the commonly used antibiotics. Erythromycin resistance has been observed worldwide, and importantly, the newer drugs such as azithromycin and clarithromycin also demonstrate a high level of microbial resistance (*11*). The structure of DesI presented here, in combination with that of PseC, provides an important molecular scaffold for the rational design of new sugar-modifying aminotransferases. By manipulating the enzymes involved in deoxysugar biosynthesis, it may be possible to produce carbohydrates with altered pharmacological properties.

MATERIALS AND METHODS

Molecular Cloning of the DesI Gene, Protein Expression, and Purification. The gene encoding DesI was PCR amplified from *S. venezuelae* genomic DNA that had been previously prepared according to published procedures (*9*). PCR primers were designed to modify the stop codon in order to produce a noncleavable C-terminally tagged protein with the sequence Gly-Leu-Glu-His_6. The PCR products were inserted into the pGEM vector (Promega) as per manufacturer's instructions. The correct open reading frame was excised from pGEM with NdeI and XhoI and inserted into pET31b(+). Chemically competent HMS 174 DE3 cells were transformed with the pET31-DesI plasmid.

The transformed cells were grown at 37 °C to an OD_{600} of 0.6 and then cooled on ice. IPTG was added to 1 mM to induce DesI production, and incubation was continued overnight at 16 °C. The cells were harvested by centrifugation, and the cell paste was flash frozen in liquid nitrogen. The frozen cells were thawed in lysis buffer (50 mM sodium

phosphate, 200 mM NaCl, 1 mM PLP, and 10 mM imidazole at pH 8.0) and disrupted by sonication at 0 °C. The remaining purification steps were conducted at 4 °C. Cellular debris was removed by centrifugation. The supernatant was passed through a Ni-NTA column (Qiagen) that was previously equilibrated with lysis buffer. After rinsing the column with lysis buffer, bound protein was eluted with a linear gradient of imidazole (10−300 mM) in the presence of 1 mM PLP, 200 mM NaCl, and 50 mM sodium phosphate at pH 8.0. Fractions containing purified DesI, as judged by SDS−PAGE, were pooled and dialyzed against standard buffer (1 mM PLP, 150 mM NaCl, and 10 mM HEPES at pH 7.5). DesI was concentrated with an Amicon Centriprep-30 ultrafiltration device to 14 mg/mL (assuming an extinction coefficient at 280 nm of 1 mg^{-1} cm^{-1} mL) and flash frozen in liquid nitrogen.

Enzymatic Synthesis of dTDP-4-amino-4,6-dideoxyglucose. dTDP-glucose was prepared by reacting glucose-1-phosphate with dTTP at 8 and 10 mM, respectively, in the presence of 2 mM $MgCl_2$, 0.15 mg/mL *E. coli* glucose-1-phosphate thymidylyltransferase, 2 units/mL inorganic pyrophosphatase from Baker's yeast, and 10 mM HEPPS, pH 8.0 at 24 °C. The protein was removed with a 30,000 molecular weight cutoff filter in an Amicon stirred cell ultra-filtration system. dTDP-glucose was then purified by anion exchange chromatography with an Amersham-Pharmacia ResourceQ column (10−300 mM ammonium carbonate gradient at pH 8.0). Fractions containing dTDP-glucose were pooled and lyophilized with a Labconco Freezone 1 lyophilizer.

dTDP-4-amino-4,6-dideoxyglucose was prepared by incubating 1 mM dTDP-glucose with 100 mM glutamate, 1 mM PLP, 1 mM EDTA, 1 mM DTT, 0.15 mg/mL DesIV, 0.15 mg/mL DesI, and 100 mM Tris, pH 7.5 at 24 °C. Protein was removed with a 10,000 molecular weight cutoff filter in an Amicon stirred cell. Purification and lyophilization were conducted as described for dTDP-glucose.

The *E. coli* glucose-1-phosphate thymidylyltransferase was a gift from Dr. James Thoden, and DesIV was prepared as previously reported (*8*). HEPPS was purchased from Research Organics, whereas all other chemicals were obtained from Sigma-Aldrich. The molecular masses of dTDP-glucose and dTDP-4-amino-4,6-dideoxyglucose were verified by ESI-MS at the University of Wisconsin Biotechnology Center. Typically, yields for the production of dTDP-4-amino-4,6-dideoxyglucose were ~95%.

Crystallization, X-ray Data Collection, and Structural Analysis. Crystallization conditions for DesI were surveyed via the hanging drop method of vapor diffusion with a sparse matrix screen designed in the laboratory. Once crystallization conditions were identified, larger yellow-tinted crystals were grown by batch methods. Specifically, equal volumes of DesI (at 14 mg/mL in standard buffer) and a precipitant solution containing 28% poly(ethylene glycol) 8000, 300 mM LiCl, 20 mM dTDP-4-amino-4,6-dideoxyglucose, and 100 mM HEPPS at pH 8.0 were mixed and subsequently centrifuged to remove any precipitated protein. The supernatant was transferred to separate wells of a batch plate, and one well was streak-seeded with DesI microcrystals obtained from the hanging drop experiments. Within several hours, visible crystals appeared at the surface of the seeded drop. These were then transferred by a loop to the unseeded wells. The crystals belonged to the space group $P2_12_12_1$ with unit cell dimensions of 59.5 Å × 66.8 Å × 242.0 Å and one dimer per asymmetric unit. Crystal dimensions were typically 1 mm × 0.6 mm × 0.2 mm.

Table 1: X-ray Data Collection and Least-Squares Refinement Statistics

resolution limits (Å)	50 − 2.1
independent relections	56057 (5602)[b]
completeness	94.9 (73.4)
redundancy	4.4 (2.9)
avg I/avg $\sigma(I)$	16.0 (2.4)
R_{sym}[a]	0.057 (0.35)
[c]R-factor (overall)%/no. of reflections	18.4/55830
R-factor (working)%/no. of reflections	18.0/50231
R-factor (free)%/no. of reflections	24.8/5599
no. protein atoms[d]	5942
No. Hetero-atoms[e]	693
weighted root-mean-square deviations from ideality	
bond lengths (Å)	0.011
bond angles (deg)	2.3
trigonal planes (Å)	0.008
general planes (Å)	0.008
torsional angles (deg)[f]	16.5

[a] $R_{sym} = (\sum|I - \bar{I}|/\sum I) \times 100$. [b] Statistics for the highest resolution bin from 2.18−2.08 Å. [c] R-factor $= (\Sigma||F_o| - |F_c||/\Sigma|F_o|) \times 100$, where F_o is the observed structure factor amplitude, and F_c is the calculated structure factor amplitude. [d] These include multiple conformations for Arg 138 in Subunit 1 and Arg 40, Gln 297, and Glu 388 in Subunit 2. [e] Heteroatoms include 2 dTDP-sugar external aldimine molecules and 593 waters. [f] The torsional angles were not restrained during the refinement.

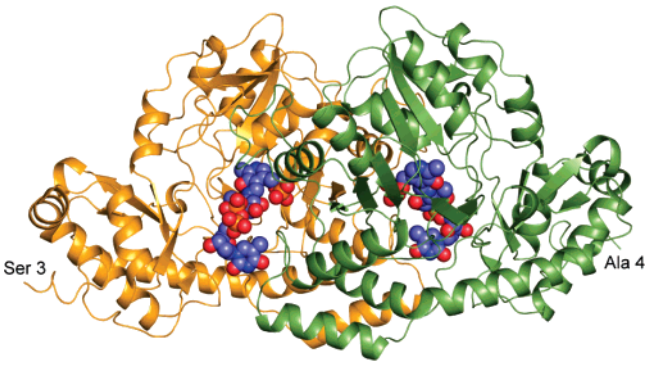

FIGURE 1: Ribbon representation of DesI. Subunits 1 and 2 in the X-ray coordinate file are color-coded in gold and green, respectively. The bound dTDP-sugar/PLP complexes are displayed in ball-and-stick representations. All figures were prepared with the software package PyMOL (*19*).

After completion of growth, the crystals were transferred to a synthetic mother liquor containing 15% poly(ethylene glycol) 8000, 100 mM NaCl, 150 mM LiCl, 0.75 mM PLP, 7 mM dTDP-4-amino-4,6-dideoxyglucose, and 50 mM HEPPS, pH 8.0 at 24 °C. Crystals were then acclimated via four incremental transfers to a cryoprotectant solution composed of 16% poly(ethylene glycol) 8000, 200 mM NaCl, 300 mM LiCl, 1 mM PLP, 10 mM dTDP-4-amino-4,6-dideoxyglucose, and 50 mM HEPPS, pH 8.0 at 24 °C. They were flash-cooled at 100 K in a nitrogen stream generated by an Oxford Cobra system.

An X-ray diffraction data set was collected from a single DesI crystal at 100 K to 2.1 Å resolution using a Bruker AXS Platinum 135 CCD detector equipped with Montel optics. CuK_α radiation was generated by a Rigaku RU200 X-ray generator operated at 50 kV and 90 mA. These data were processed with SAINT (Bruker AXS) and internally

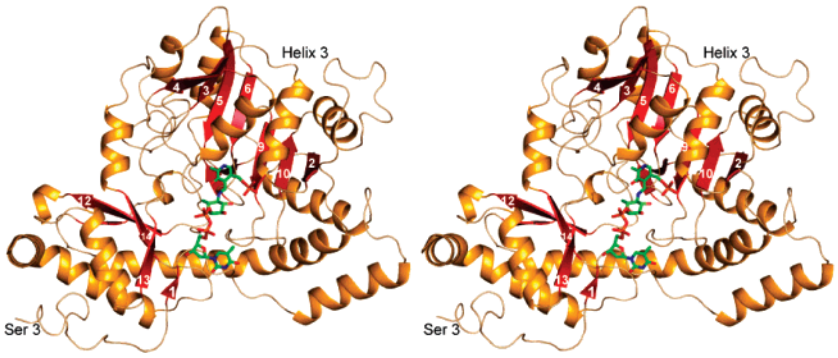

FIGURE 2: Overall structure of Subunit 1. A stereo ribbon representation of the DesI subunit is displayed with the β-strands numbered and highlighted in red.

Scheme 2

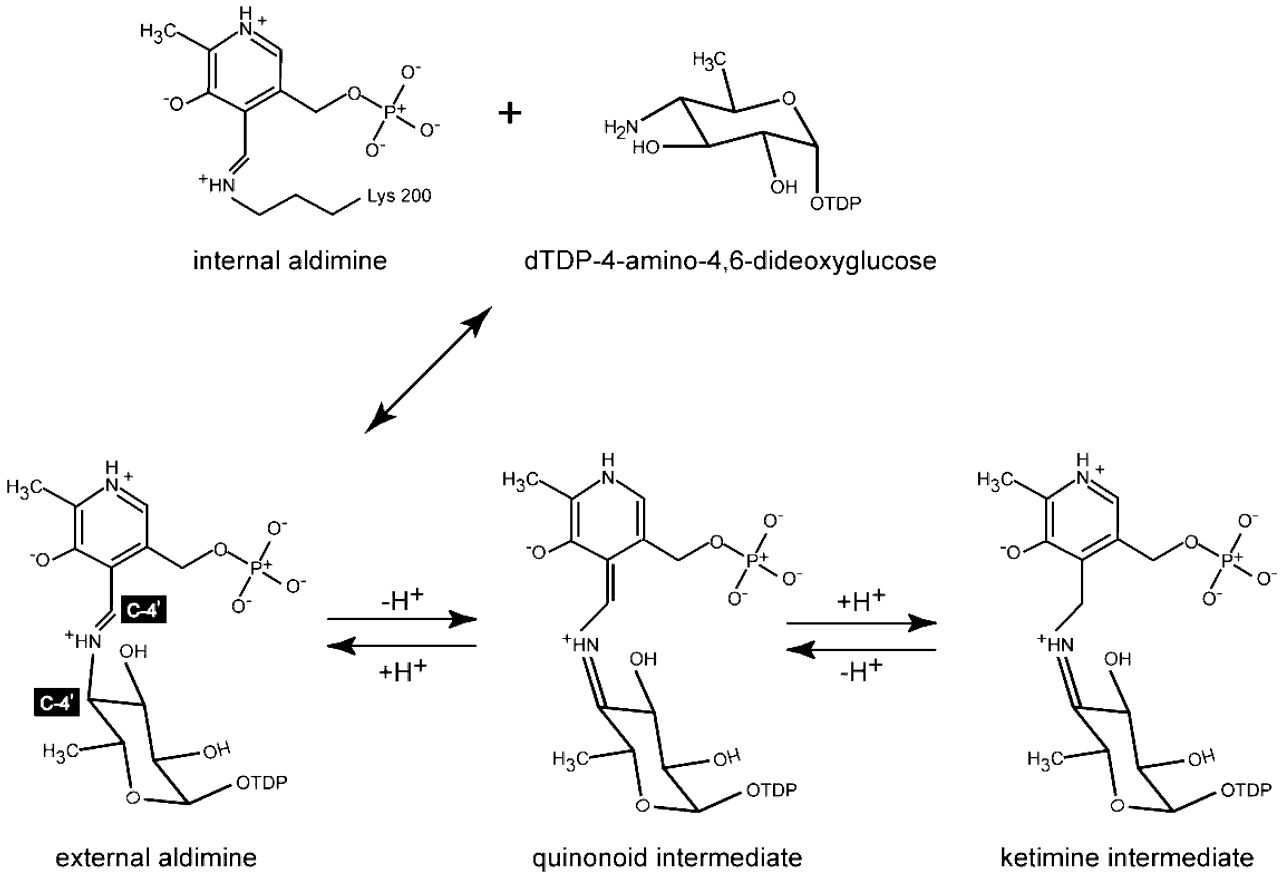

scaled with SADABS (Bruker AXS). X-ray data collection statistics are presented in Table 1.

A polyalanine model of DesV (pdb accession code 2OGA) (*9*) was used as a search model to solve the structure of DesI by molecular replacement with the software package PHASER (*12*, *13*). The model was manually built with TURBO. Alternate cycles of least-squares refinement with the software package TNT (*14*) and manual rebuilding reduced the overall *R*-factor to 18.4% for all measured X-ray data. Relevant refinement statistics are presented in Table 1.

RESULTS AND DISCUSSION

Overall Structure of DesI. The crystals of DesI employed in this structural analysis belonged to the space group $P2_12_12_1$ with one dimer in the asymmetric unit. The electron density for Subunit 1 was continuous from Ser 3 to Asp 395, whereas that for Subunit 2 was continuous from Ala 4 to Asp 395. In both subunits, the last 20 C-terminal residues were disordered, and the electron density for the region defined by Gly 13 to Pro 20 in Subunit 2 was weak. Overall, the quality of the refined model was excellent with 88.3% and 11.3% of the dihedral angles located within the core and allowed regions, respectively, of the Ramachandran plot. The only significant outlier in each subunit was Phe 205 (ϕ = 81.4°, ψ = −68.9° in Subunit 1 and ϕ = 73.3°, ψ = −63.8° in Subunit 2). It should be noted, however, that the electron densities for these residues were unambiguous in both subunits. Phe 205 is situated within ~8 Å from the thymine base of the ligand. The corresponding residue in PseC is Ala 188, which also adopts similar dihedral angles. Each subunit of DesI contains three cis-peptides in near proximity: Phe 330, Pro 332, and Pro 339. In PseC, the homologous residue

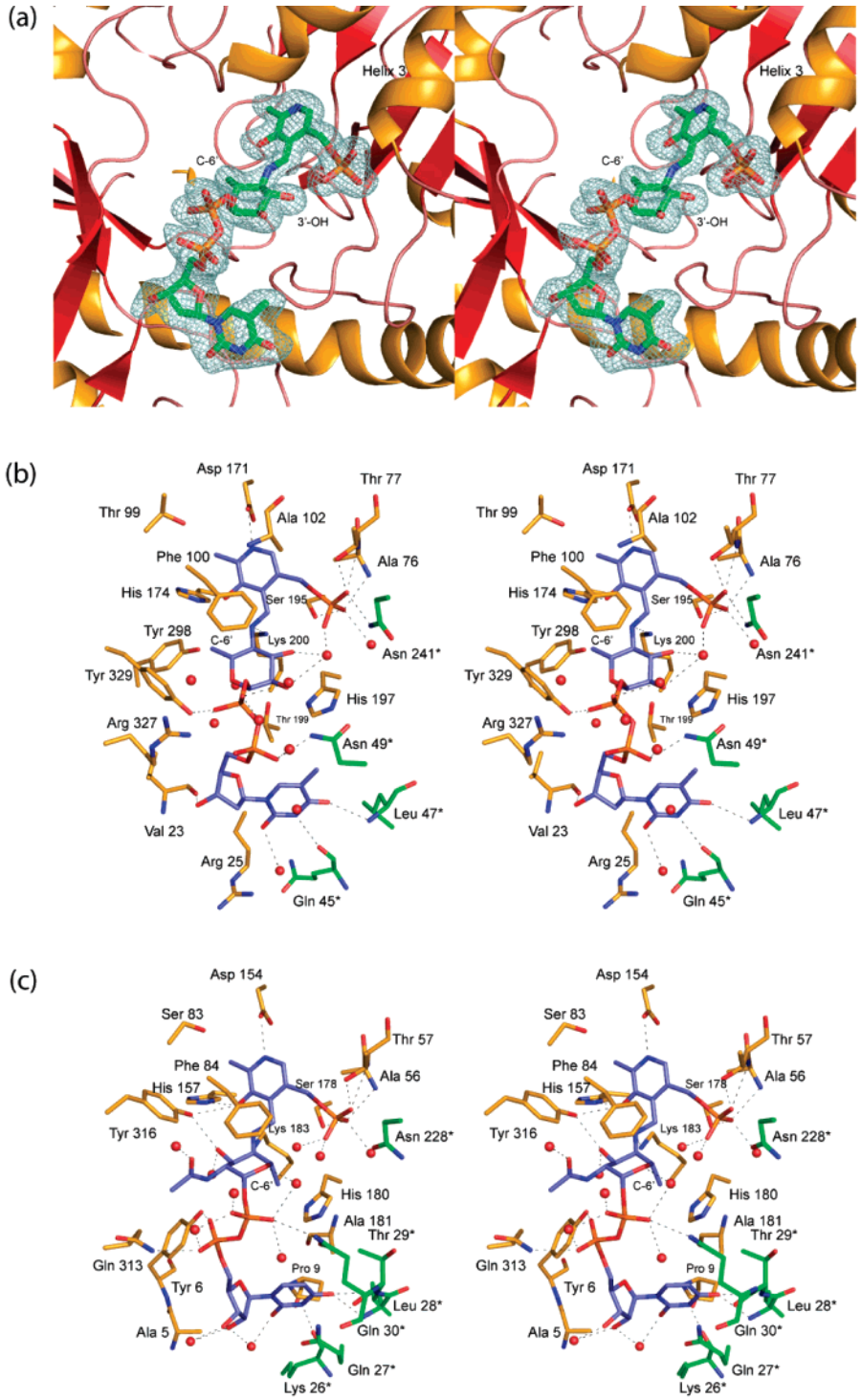

FIGURE 3: Active site of DesI. Electron density corresponding to the external aldimine is shown in (a). The map was calculated with coefficients of the form ($F_o - F_c$), where F_o was the native structure factor amplitude, and F_c was the calculated structure factor amplitude with the atoms corresponding to external aldimine excluded from the calculation. The map was contoured at 3σ. Those amino acid residues located within ~3.5 Å of the ligand are shown in (b). Residues highlighted in green bonds and marked by an asterisk belong to Subunit 2. Possible hydrogen bonds (3.2 Å) are indicated by the dashed lines. Note that the electron density for Arg 327 was weak, and its position in the active site is tentative. Consequently, it may or may not interact with the α-phosphoryl oxygens of the ligand. The corresponding active site pocket for PseC is shown in (c). Coordinates were obtained from the protein data bank (accession no. 2FNU). The color coding is the same as that described in (b).

for Phe 330 is Tyr 316, which also adopts the cis configuration and hydrogen bonds to a sugar hydroxyl as discussed later. Interestingly, Pro 332 in DesI corresponds to Pro 318 in PseC, which in this case is in the trans conformation. Finally, Pro 339 in DesI is not conserved in PseC but rather is a leucine residue.

DesI belongs to the aspartate aminotransferase family. Enzymes in this group are typically homodimers and contain two key features: a PLP cofactor attached to a lysine via a Schiff base and an aspartate that promotes protonation of the PLP ring nitrogen to enhance its electron sink properties (*15*, *16*). These correspond to Lys 200 and Asp 171 in DesI.

Scheme 3

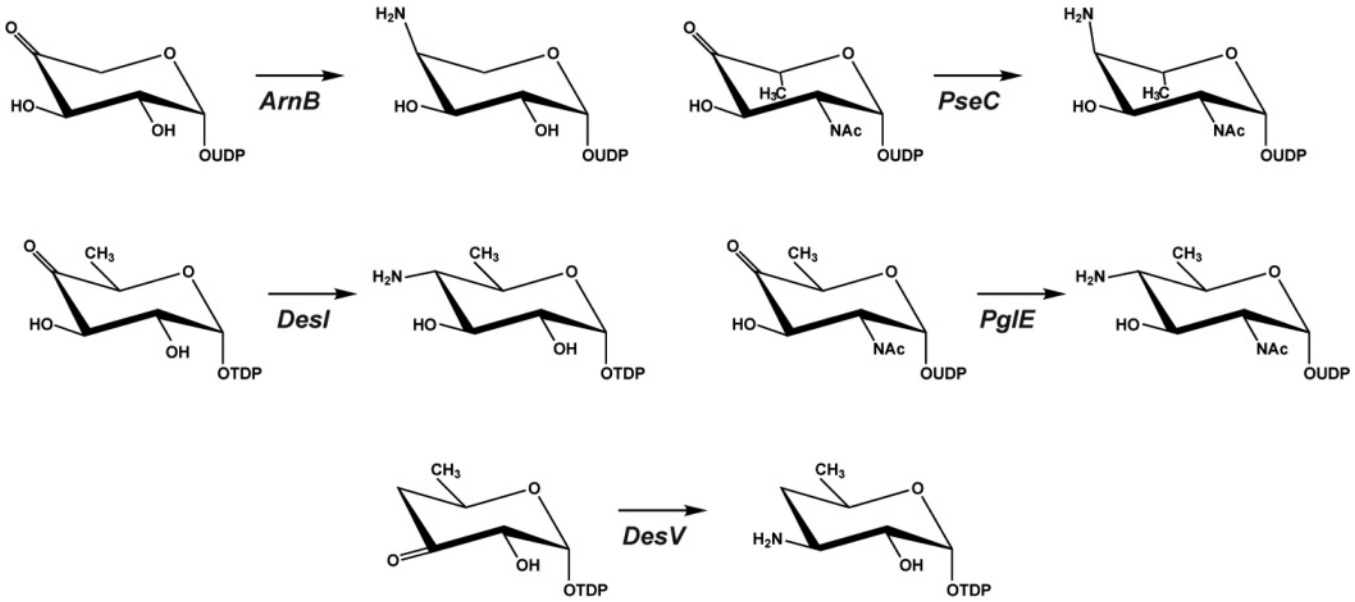

As can be seen by the ribbon representation in Figure 1, the DesI dimer has an extensive subunit/subunit interface. Specifically, the total buried surface area is 4500 Å^2. The interface is formed primarily by Arg 25 to Asn 49 (helix 1), Asn 75 to His 85 (helix 3), Phe 100 to Ile 110 (helix 4), Phe 205 to Glu 206, Leu 224 to Phe 229, and Ser 235 to Ala 247. A combination of aromatic stacking interactions and salt bridges contribute to the interface. Examples include stacking interactions between His 85 and Trp 109*, Tyr 35 and Tyr 35*, and Phe 100 and Phe 227*, and salt bridges between Arg 31 and Asp 43* and Glu 206 and Lys 243* (where the asterisk indicates the second subunit of the dimer). The two active sites of DesI are widely separated by ~29 Å.

Given that the α-carbons for the two subunits of the DesI dimer superimpose with a root-mean-square deviation of 0.31 Å, the following discussion refers only to Subunit 1 unless otherwise noted. A ribbon representation of this subunit is presented in Figure 2. The overall architecture of the subunit is built around 12 α-helices and 14 β-strands. Seven of the β-strands (β-strands 2, 3, 4, 5, 6, 9, and 10) form a large mixed β-sheet, which is flanked on each side by three α-helices. In addition to this large mixed β-sheet, there are three additional layers of β-sheet: a two-stranded parallel sheet (β-strands 1 and 13), a two-stranded antiparallel sheet (β-strands 7 and 8), and a three-stranded antiparallel sheet (β-strands 11, 12, and 14). Helix 3, formed by Ala 76 to Ala 86, is situated with the positive end of its helix dipole moment projecting toward the phosphate group of PLP. The 12 α-helices in the subunit range in size from 4 to 31 residues with the C-terminal α-helix, formed by Asp 369 to Asp 395, displaying a decidedly sharp bend. This kink is a result of Arg 385 adopting dihedral angles of $\phi = -127°$ and $\psi = 17°$.

Active Site Containing the External Aldimine Intermediate. In the resting state, the PLP cofactor is attached to DesI via a Schiff base with the ϵ-amino group of Lys 200 (Scheme 2). This is referred to as the internal aldimine. For the structural analysis presented here, DesI was crystallized in the presence of its product, dTDP-4-amino-4,6-dideoxy-glucose. Apparently the reaction is reversible because, as can be seen from the electron density displayed in Figure 3a, the amino group of the product forms a covalent bond with the C-4′ atom of PLP. The formation of this covalent bond displaces Lys 200 and yields what is believed to be the external aldimine. It should be noted, however, that the external aldimine can further react to yield the resonance-stabilized quinonoid followed by the ketimine intermediate as highlighted in Scheme 2. The major structural difference between the external aldimine and the quinonoid intermediate occurs at the sugar C-4′ where in the former, the carbon is sp^3 hybridized, and in the latter, it assumes sp^2 hybridization. Likewise, the main structural difference between the quinonoid intermediate and the ketimine intermediate is at C-4′ of the pyridoxal ring where in the former, it is sp^2 hybridized, and in the latter, it is sp^3 hybridized. Although the electron density appears to accommodate the external aldimine intermediate most easily, at a resolution of 2.1 Å, the presence of the ketimine intermediate cannot be ruled out.

A stereoview of the hydrogen-bonding pattern surrounding the PLP and dTDP-sugar in Subunit 1 is presented in Figure 3b. The thymine ring of the product is anchored to the protein through interactions with the backbone carbonyl oxygen of Gln 45 and the backbone amide nitrogen of Leu 47, both contributed by Subunit 2. The carboxamide group of Asn 49 from Subunit 2 interacts with an α-phosphoryl oxygen of the dTDP-sugar. An additional side chain from Subunit 1, Tyr 329, lies within 3.2 Å from a β-phosphoryl oxygen of the product. The backbone carbonyl oxygen of Val 23 hydrogen bonds with the 3-hydroxyl group of the ribose. The PLP moiety is held in place primarily through side chain interactions with Thr 77, Asp 171, His 174, and Ser 195 in Subunit 1 and Asn 241 in Subunit 2. In addition, the backbone amide groups of Ala 76 and Thr 77 participate in hydrogen bonds with the phosphoryl group of the cofactor. N$^\zeta$ of Lys 200 is situated at 2.9 Å from the Schiff base nitrogen of the trapped intermediate. Numerous water molecules line the active site cleft.

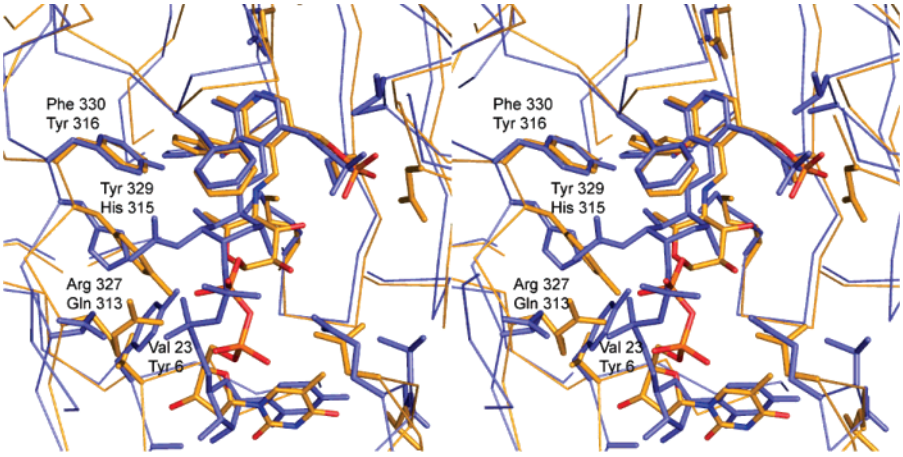

FIGURE 4: Comparison of the active site regions for DesI and PseC. Those residues belonging to DesI are depicted in gold whereas those for PseC are displayed in slate. The top and bottom labels refer to residues in DesI and PseC, respectively.

Comparison with PseC. To date, four other X-ray crystallographic structures of sugar-modifying aminotransferases have been determined: (1) ArnB from *Salmonella typhimurium*, a 4-amino-4-deoxy-L-arabinose lipopolysaccharide-modifying enzyme (*17*), (2) PseC, an aminotransferase from *H. pylori* that is involved in the biosynthesis of pseudaminic acid (*10*), (3) PglE, an enzyme responsible for amino transfer in the production of UDP-2,4-diacetamido-2,4,6,trideoxy-α-D-glucopyranose in *Campylobacter jejuni* (*18*), and (4) DesV, the second aminotransferase in the desosamine biosynthetic pathway (*9*). The reactions catalyzed by these enzymes are presented in Scheme 3. ArnB, PseC, PglE, and DesI catalyze the amination of the sugar C-4′, whereas DesV acts on C-3′ of the hexose. As might be expected, the overall three dimensional folds for these enzymes are similar. The details in their active site pockets, however, are what allow these enzymes to function on different hydroxyl positions and/or to transfer amino groups to either the equatorial or axial positions.

At present, the only other sugar-modifying aminotransferase whose structure has been solved with a bound sugar ligand is PseC. Both DesI and PseC catalyze aminations at the sugar C-4. However, in the reaction catalyzed by PseC, the amino group is transferred to the axial position, whereas in DesI, the transfer results in an equatorial orientation for the amino group. A close-up view of the PseC active site with bound product (UDP-4-amino-4,6-dideoxy-β-L-AltNAc) is displayed in Figure 3c. The immediate protein environment surrounding the pyridoxal cofactor in PseC is strikingly similar to that observed in DesI, including the hydrogen-bonding interactions with Ala 56, Thr 57, Asp 154, His 157, and Ser 178. In both enzymes, there is an interaction between the hexose and a phenylalanine side chain (Phe 100 in DesI and Phe 84 in PseC). As observed in DesI, in PseC the uracil ring hydrogen bonds with only backbone atoms contributed by the second subunit of the dimer. The major differences in ligand binding between PseC and DesI are in the orientations of the glucosyl and phosphoryl groups as highlighted in Figure 4. The nearly 180° difference in hexose orientation arises from changes in the dihedral angles about the phosphoryl groups of the nucleotide-linked sugars. The difference in stereochemistry between the PseC and DesI reactions, axial versus equatorial amino transfer, respectively, is due to the flip in orientation of the hexose ring. The structural factors that drive the differences in ligand binding are not entirely clear at this point. The 3′-hydroxyl group of the hexose in the PseC model (Figure 3c) hydrogen bonds with the side chain of Tyr 316, and this side chain is a phenylalanine in DesI (Phe 330), thereby precluding such an interaction. If the hydrogen bond between the tyrosine residue and the 3′-hydroxyl group of the sugar functions to drive the hexose into the orientation observed for PseC, then it would be expected that ArnB another enzyme catalyzing axial amino transfer would also contain a tyrosine residue in this position. But, in fact, the homologous residue in ArnB is a phenylalanine. Thus, the differences in stereochemistry likely arise from a combination of subtle structural factors, especially those that act to orient the phosphoryl groups of the nucleotide-linked sugars into the active sites of their respective proteins. Understanding these differences will require further structural analyses of additional enzyme/product complexes. This work is in progress.

ACKNOWLEDGMENT

We gratefully acknowledge Drs. James B. Thoden, W. W. Cleland, and Mr. Paul D. Cook for helpful discussions.

REFERENCES

1. Schlunzen, F., Zarivach, R., Harms, J., Bashan, A., Tocilj, A., Albrecht, R., Yonath, A., and Franceschi, F. (2001) Structural basis for the interaction of antibiotics with the peptidyl transferase centre in eubacteria, *Nature 413*, 814−821.
2. Hansen, J. L., Ippolito, J. A., Ban, N., Nissen, P., Moore, P. B., and Steitz, T. A. (2002) The structures of four macrolide antibiotics bound to the large ribosomal subunit, *Mol. Cell 10*, 117−128.
3. Schlunzen, F., Harms, J. M., Franceschi, F., Hansen, H. A., Bartels, H., Zarivach, R., and Yonath, A. (2003) Structural basis for the antibiotic activity of ketolides and azalides, *Structure 11*, 329−338.
4. Zhanel, G. G., Walters, M., Noreddin, A., Vercaigne, L. M., Wierzbowski, A., Embil, J. M., Gin, A. S., Douthwaite, S., and Hoban, D. J. (2002) The ketolides: a critical review, *Drugs 62*, 1771−1804.
5. He, X. M., and Liu, H. W. (2002) Formation of unusual sugars: mechanistic studies and biosynthetic applications, *Annu. Rev. Biochem. 71*, 701−754.
6. Rupprath, C., Schumacher, T., and Elling, L. (2005) Nucleotide deoxysugars: essential tools for the glycosylation engineering of novel bioactive compounds, *Curr. Med. Chem. 12*, 1637−1675.
7. Nedal, A., and Zotchev, S. B. (2004) Biosynthesis of deoxyaminosugars in antibiotic-producing bacteria, *Appl. Microbiol. Biotechnol. 64*, 7−15.

8. Allard, S. T., Cleland, W. W., and Holden, H. M. (2004) High resolution X-ray structure of dTDP-glucose 4,6-dehydratase from *Streptomyces venezuelae*, *J. Biol. Chem. 279*, 2211−2220.
9. Burgie, E. S., Thoden, J. B., and Holden, H. M. (2007) Molecular architecture of DesV from *Streptomyces venezuelae*: a PLP-dependent transaminase involved in the biosynthesis of the unusual sugar desosamine, *Protein Sci. 16*, 887−896.
10. Schoenhofen, I. C., Lunin, V. V., Julien, J. P., Li, Y., Ajamian, E., Matte, A., Cygler, M., Brisson, J. R., Aubry, A., Logan, S. M., Bhatia, S., Wakarchuk, W. W., and Young, N. M. (2006) Structural and functional characterization of PseC, an aminotransferase involved in the biosynthesis of pseudaminic acid, an essential flagellar modification in *Helicobacter pylori*, *J. Biol. Chem. 281*, 8907−8916.
11. Hoban, D. J., Doern, G. V., Fluit, A. C., Roussel-Delvallez, M., and Jones, R. N. (2001) Worldwide prevalence of antimicrobial resistance in *Streptococcus pneumoniae*, *Haemophilus influenzae*, and *Moraxella catarrhalis* in the SENTRY Antimicrobial Surveillance Program, 1997−1999, *Clin. Infect. Dis. 32*, S81−S93.
12. Storoni, L. C., McCoy, A. J., and Read, R. J. (2004) Likelihood-enhanced fast rotation functions, *Acta Crystallogr., Sect. D 60*, 432−438.
13. McCoy, A. J., Grosse-Kunstleve, R. W., Storoni, L. C., and Read, R. J. (2005) Likelihood-enhanced fast translation functions, *Acta Crystallogr., Sect. D 61*, 458−464.
14. Tronrud, D. E., Ten Eyck, L. F., and Matthews, B. W. (1987) An efficient general-purpose least-squares refinement program for macromolecular structures, *Acta Crystallogr., Sect. A 43*, 489−501.
15. Eliot, A. C., and Kirsch, J. F. (2004) Pyridoxal phosphate enzymes: mechanistic, structural, and evolutionary considerations, *Annu. Rev. Biochem. 73*, 383−415.
16. Paiardini, A., Bossa, F., and Pascarella, S. (2004) Evolutionarily conserved regions and hydrophobic contacts at the superfamily level: the case of the fold-type I, pyridoxal-5′-phosphate-dependent enzymes, *Protein Sci. 13*, 2992−3005.
17. Noland, B. W., Newman, J. M., Hendle, J., Badger, J., Christopher, J. A., Tresser, J., Buchanan, M. D., Wright, T. A., Rutter, M. E., Sanderson, W. E., Muller-Dieckmann, H. J., Gajiwala, K. S., and Buchanan, S. G. (2002) Structural studies of *Salmonella typhimurium* ArnB (PmrH) aminotransferase: a 4-amino-4-deoxy-L-arabinose lipopolysaccharide-modifying enzyme, *Structure (London) 10*, 1569−1580.
18. Schoenhofen, I. C., McNally, D. J., Vinogradov, E., Whitfield, D., Young, N. M., Dick, S., Wakarchuk, W. W., Brisson, J. R., and Logan, S. M. (2006) Functional characterization of dehydratase/aminotransferase pairs from *Helicobacter* and *Campylobacter*: enzymes distinguishing the pseudaminic acid and bacillosamine biosynthetic pathways, *J. Biol. Chem. 281*, 723−732.
19. DeLano, W. L. (2003) *PyMOL*, DeLano Scientific LLC, Palo Alto, CA.

BI700751D